SUPPLEMENTARY INFORMATION

Coprinopsis cinerea uses laccase Lcc9 as a defense strategy to eliminate oxidative stress during fungal-fungal interactions

Juanjuan Liu[a,b,c], Can Peng[a,b,c], Qiqi Han[a,b,c], Mengyao Wang[a,b,c], Gang Zhou[a,b,c], Bin Ye[a], Yazhong Xiao[a,b,c], Zemin Fang[a,b,c*], Ursula Kües[d*]

a, School of Life Sciences, Anhui University;

b, Anhui Key Laboratory of Modern Biomanufacturing;

c, Anhui Provincial Engineering Technology Research Center of Microorganisms and Biocatalysis, Hefei, Anhui 230601, China

d, Büsgen-Institut, Molecular Wood Biotechnology and Technical Mycology and Goettingen Center for Molecular Biosciences (GZMB), University of Goettingen, Büsgenweg 2, 37077, Goettingen, Germany

* Corresponding author

Phone/Fax: +86-551-63861063

E-mail: zemin_fang@ahu.edu.cn (to ZF); ukuees@gwdg.de (to UK)

Supplementary Methods

GC-MS analysis of compounds in *Gongronella* sp. w5 culture broth

The ether-extracted organic metabolites from 1 L SAHX (plus sucrose) culture broth of actively growing *Gongronella* sp. w5 after 60 h cultivation were concentrated, re-dissolved in methanol, and applied to gas chromatography-mass spectrometry (GC-MS) analysis. The chromatographic conditions were as follows: Agilent HP-5MS column (300 mm × 0.32 mm × 0.25 μm, Bio-Rad, Hercules, CA, USA), with helium as the mobile phase, with a flow rate of 1.2 mL/min. The mass spectrometry library used was NIST05a.L.

Construction and screening of *lcc9* silencing transformants

lcc9 antisense silencing fragments were inserted into plasmid pYSK7 [1] through homologous recombination in the yeast *Saccharomyces cerevisiae* Y1HGold. Two distinct silencing fragments were designed. *lcc9* antisense silencing fragments were amplified using primers listed in Table S1 for *in vivo*-cloning, giving *lcc9* silencing plasmid pYSK-*lcc9*-antisense-1 and pYSK-*lcc9*-antisense-2, respectively. Plasmids from yeast transformants were extracted and amplified in *Escherichia coli* for DNA sequencing [2].

Transformation of the *lcc9* silencing plasmids into *C. cinerea* protoplasts was performed exactly as described by Dörnte and Kües (2012) [3]. Briefly, protoplasts were co-transformed with a pYSK-*lcc9*-antisense plasmid and the selection vector p*Cc*Ade8 with the *C. cinerea ade8*$^{+}$ gene [2] and transformants were selected on regeneration medium for growth without adenine. Clones were further verified based on PCR amplification of *gpdII* promoter-*lcc9* antisense-*lcc1* terminator fragments from the genome of transformants using primers listed in Table S3 [2].

Sequence alignments of *lcc1*, *lcc5*, and *lcc9* was performed using software Clustal Omega

(https://www.ebi.ac.uk/Tools/msa/clustalo/) to select proper target antisense fragments and avoid similar regions of *lcc9* to *lcc1* and *lcc5* [2].

Mycelial growth and morphology assay on agar plates

C. cinerea wild-type and *lcc9* silencing strains were inoculated in single culture with small mycelial plugs onto solid SAHX plates using fructose as the sole carbon source and incubated at 37 °C. For coculture of *C. cinerea* strains with *Gongronella* sp. w5, sucrose was substituted for fructose and used as the carbon source. The initial distance between inocula of *C. cinerea* and *Gongronella* sp. w5 on plates was about 5 cm. All colonies for three parallel agar plates were photographed and measured every 24 h to evaluate the mycelial growth rates of the strains. The pictures were transformed to grey- scale map and the colony areas were calculated by pixel scale using Matlab software.

Morphology of *C. cinerea* wild-type or *lcc9* silencing strains was assayed by inoculating *C. cinerea* strains and *Gongronella* sp. w5 on opposite sides of SAXH solid medium with sucrose loaded on microscope slides (Fig. S2A). For morphology observation of single-species cultured *C. cinerea*, SAXH solid medium with fructose was used. The hyphae of *C. cinerea* were then observed under a ZEISS AXIO Scope A1 microscope (ZEISS, Oberkochen, Germany). Images were captured with an Axiocam 506 color digital camera (Zeiss) under bright field illumination and processed with Adobe Photoshop 7.0 software (Adobe Inc., San Jose, CA).

For transmission electron microscopy (TEM) observation, mycelial liquid culture samples were fixed in 2.5% glutaraldehyde and 1% OsO_4 and then dehydrated with ethanol. The samples were infiltrated with propylene oxide and Araldite resin (1:1, v/v), and polymerized in Araldite resin (Araldite resin CY-212, Poly/Bed 812, DDSA, DMP-30) at 60 °C for 72 h. Cured blocks were

trimmed and thin-sectioned with a diamond knife on an EM KMR microtome (Leica Microsystems Wetzlar GmbH, Germany). The samples were examined with a Hitachi H800 transmission electron microscope (HITACHI, Tokyo, Japan).

Spore counting

C. cinerea wild-type or *lcc9* silencing strains and *Gongronella* sp. w5 were inoculated about 5 cm distant from each other on SAXH plates with sucrose as carbon source and cultured in the dark at 37 °C for 7 days for abundant constitutive oidia production [4, 5]. The spores of the entire *C. cinerea* colonies were harvested from plates in sterile water by scraping the mycelium and were then counted using a haematocytometer.

Reference

[1] Kilaru, S., Hoegger, P. J., Majcherczyk, A., Burns, C., Shishido, K., Bailey, A., *et al*. 2006. Expression of laccase gene *lcc1* in *Coprinopsis cinerea* under control of various basidiomycetous promoters. Appl Microbiol Biotechnol 71: 200-210.

[2] Dörnte, B., Kües, U. 2012. Reliability in transformation of the basidiomycete *Coprinopsis cinerea*. Curr Trends Biotechnol Pharm 6:340-355.

[3] Dörnte, B., Peng, C., Fang, Z., Kamran, A., Yulzivar, C., Kües, U. 2020. Selection markers for transformation of the sequenced reference monokaryon Okayama 7/#130 and homokaryon AmutBmut of *Coprinopsis cinerea.* Fungal Biol Biotechnol 7: 15.

[4] Kertesz-Chaloupková K, Walser PJ, Granado JD, Aebi M, Kües U. 1998. Blue light overrides repression of asexual sporulation by mating type genes in the basidiomycete *Coprinus cinereus*. Fungal Genet Biol 23(1): 95-109.

[5] Kües U, Granado JD, Hermann R, Boulianne RP, Kertesz-Chaloupková K, Aebi M. 1998. The A mating type and blue light regulate all known differentiation processes in the basidiomycete *Coprinus cinereus*. Mol Gen Genet 260(1): 81-91.

[6] Hu J, Zhang Y, Xu Y, Sun Q, Liu J, Fang W, Xiao Y, Kües U, Fang Z. 2019. G*ongronella* sp. w5 elevates *Coprinopsis cinerea* laccase production by carbon source syntrophism and secondary metabolite induction. Appl Microbiol Biotechnol 103(1): 411-425.

[7] D'Autréaux B, Toledano MB. 2007. ROS as signalling molecules: mechanisms that generate specificity in ROS homeostasis. Nat Rev Mol Cell Bio 8(10): 813-824.

[8] Basso V, Znaidi S, Lagage V, Cabral V, Schoenherr F, Leibundgut-Landmann S, d'Enfert C, Bachellier-Bassi S. 2017. The two-component response regulator Skn7 belongs to a network of transcription factors regulating morphogenesis in *Candida albicans* and independently limits morphogenesis-induced ROS accumulation. Mol Microbiol 106(1): 157-182.

Supplementary Tables and Figures

Table S1 Transcripts in many pathways were shown to be significantly enriched with a cutoff value of *P* value ≤ 0.05 and *FDR* ≤ 0.05. All enriched pathways are presented in Table S1-1. Genes involved in primary metabolic pathways, genes involved in oxidative stress response, genes involved in sesquiterpene synthesis and siderophore production, genes of transcription factors, and genes involved in cell wall synthesis are listed in Tables S1-2 to S1-6.

Please see separated data set “Table S1”.

Retention time/min	Compound	MW /U
7.288	Benzeneacetic acid	136
8.903	4-Hydroxy-benzaldehyde	122
9.063	9-Decenoic acid	170
9.126	4-Hydroxy-benzenepropanoic acid	180
10.121	2,3-Dimethyl-naphthalene	156
12.204	2,6-Dimethyl-naphthalene	156
10.564	Dimethyl phthalate	194
10.735	1,4-Dimethyl-naphthalene	156
10.793	3-Hydroxy-decanoic acid methyl ester	202
11.132	4-Hydroxy-benzeneacetic acid methyl ester	166
11.233	3-Methyl-1,1'-biphenyl	168
11.375	4-Methyl-1,1'-biphenyl	168
11.532	2,3,6-Trimethyl-naphthalene	170
11.808	1,6,7-Trimethyl-naphthalene	170
11.896	2,3,6-Trimethyl-naphthalene	170
12.009	1-Methyl-4-(phenylmethyl)-benzene	182
12.081	1,6,7-Trimethyl-naphthalene	170
12.583	Fluorene	166
12.642	3,3'-Dimethylbiphenyl	182
12.768	4,4'-Dimethylbiphenyl	182
12.955	1-Methyl-2-[(3-methylphenyl)methyl]-benzene	196
13.069	2,2'-Dimethylbiphenyl	182
13.143	1,1'-Methylenebis(4-methyl)-benzene	196
13.296	(E)-1,2,3-Trimethyl-4-propenyl-naphthalene	210
13.386	(E)-1,2,3-Trimethyl-4-propenyl-naphthalene	210
13.561	2,2’,5,5’-Tetramethyl-1,1'-biphenyl	210
13.605	2,2',5,5'-Tetramethyl-1,1'-biphenyl	210
13.669	(E)-1,2,3-Trimethyl-4-propenyl-naphthalene	210
13.896	Bis-(2-methoxyethyl)-amine	133
13.984	2,2',5,5'-Tetramethyl-1,1'-biphenyl	210
14.142	2-Phenyl-3-(4-methylphenyl)-oxirane	210
14.200	1,2,3,4-Tetrahydro-9-propyl-anthracene	224
14.465	1,2,3,4-Tetrahydro-9-propyl-anthracene	224
14.523	3,5,3',5'-Tetramethylbiphenyl	210
14.614	Anthracene	178
14.866	2,3-Dimethyl-9-fluorene	194
15.008	1,4,7-Trimethyl-2-azafluorene	209
15.520	2-Dodecylcyclobutanone	238
15.895	Cis-9-hexadecenal	238
15.998	n-Hexadecanoic acid	256
17.518	Cycloundecanone	168
17.971	Octadecanoic acid	284
18.152	Hexadecanamide	225
19.938	(Z)-9-Octadecenamide	281
20.229	Octadecanamide	283
20.513	2,2'-Methylenebis[6-(1,1-dimethylethyl)-4-methyl]-phenol	340

Table S2 Metabolites of *Gongronella* sp. w5 detected by GC-MS in culture broth.

Wild-type	R2-11	R2-19	R2-23
2×10^8	2×10^7	8×10^6	3×10^7

Table S3 Mitotic spores of the wild-type and three *lcc9* silencing strains.

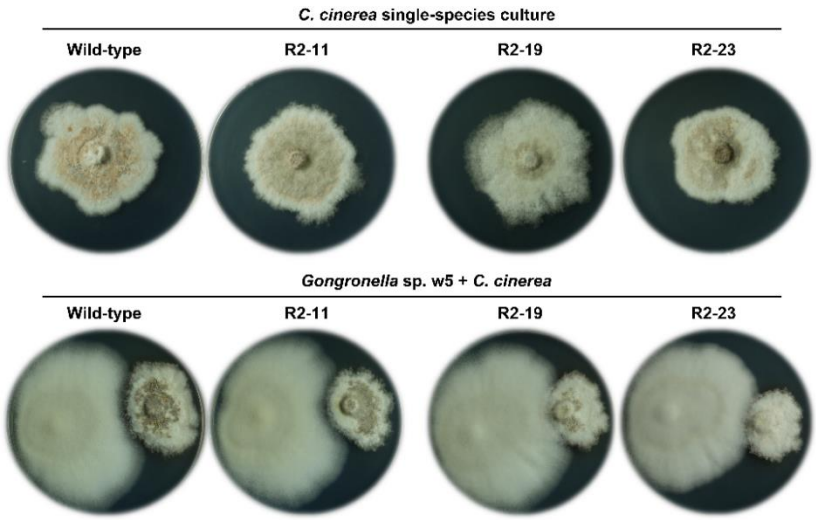

Figure S1 Laccase *lcc9* silencing affected the hyphal growth of *C. cinerea* during confrontation culture with *Gongronella* sp. w5 but not in single-species culture.

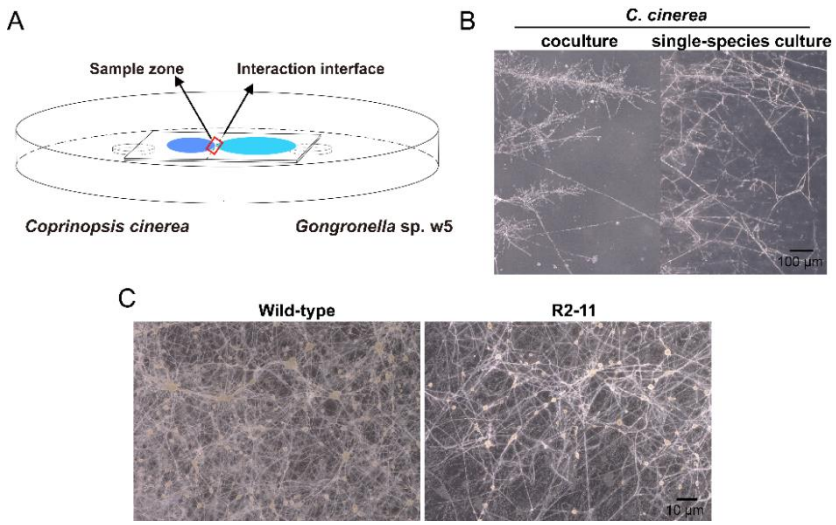

Figure S2 Lcc9 was involved in cell morphology of *C. cinerea* in coculture with *Gongronella* sp. w5. (A), Scheme of the cell morphology assay on microscope slides of the wild-type or *lcc9* silencing strains in interaction with *Gongronella* sp. w5. (B), The short hyphal branches of mycelial growth fronts in *C. cinerea*. The left panel showed the interspecific region in coculture, and the right panel showed the marginal region in single-species culture. (C), Mycelium morphology and the distribution of oidia collected in droplets in the aerial mycelium of *C. cinerea* wild-type strain and *lcc9* silencing strain R2-11.

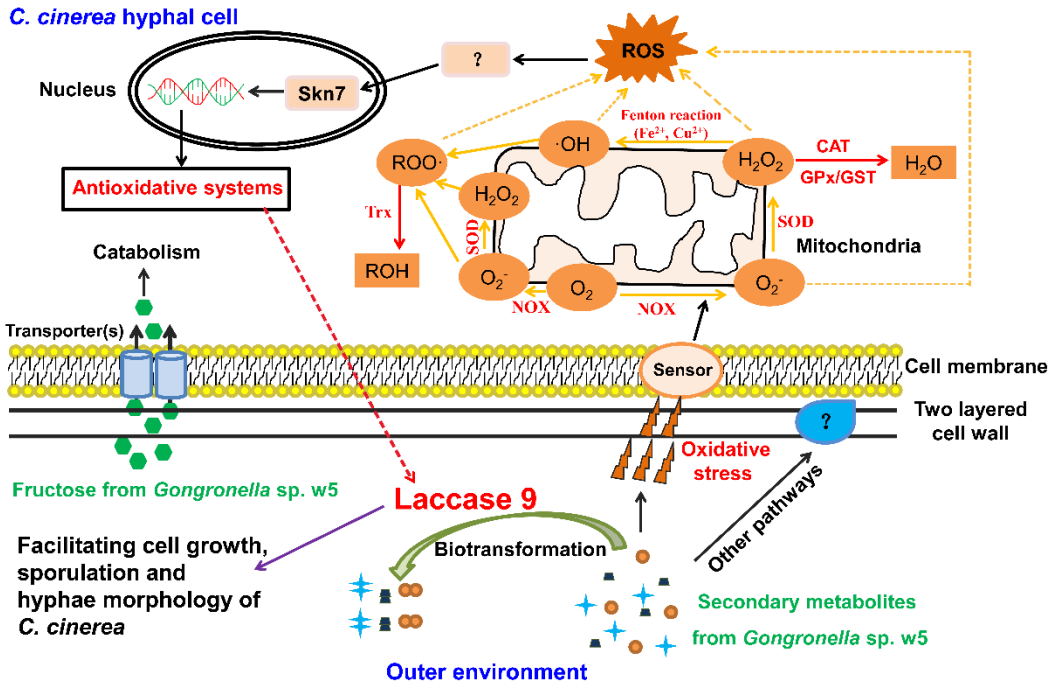

Figure S3 Model for a possible link between ROS and Lcc9 in *C. cinerea*. Specific utilization of fructose as carbon energy source and oxidative stress caused by toxic metabolites from *Gongronella* sp. w5 contributed to Lcc9 activation in *C. cinerea* (Hu et al. 2019 [6] and this study), mediated by a signal transduction system from the membrane to the nucleus under intracellular production of types of ROS (D'Autréaux and Toledano, 2007 [7]) and activation of antioxidant systems including extracellular laccase and various intracellular antioxidant proteins induced by direct or indirect action of the oxidative stress transcription factor Skn7 (Basso et al. 2017 [8]). Produced laccase 9 positively influences cell growth, sporulation and hyphal morphology by reducing the oxidative stress, possibly by biotransformation of the extracellular toxic metabolites from *Gongronella* sp. w5. ROS, reactive oxygen species; NOX, NADPH (nicotinamide adenine dinucleotide phosphate) oxidase; SOD, superoxide dismutase; CAT, catalase; GPx, glutathione peroxidase; GST, glutathione S-transferase; Trx, thioredoxin; ROOH, organic peroxides. Black arrows, signal transduction; orange arrows, oxidative stress induced ROS generation; red arrows and words, ROS elimination; purple arrows, the functions of Lcc9.

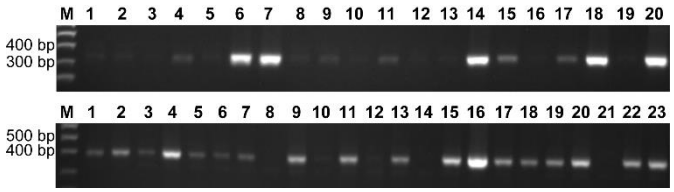

Figure S4 Positive transformants were verified by PCR amplification of *gpdII* promoter-*lcc9* antisense-*lcc1* terminator fragments from their genomes. (A) Twenty transformants of pYSK- *lcc9* antisense 1 were analyzed. (B) Twenty three transformants of pYSK- *lcc9* antisense 2 were analyzed. Primers used were PF and PR listed in Table 1.